Two-dimensional electron-hole system in a strong magnetic field as an almost ideal exciton gas

I. V. Lerner and Yu. E. Lozovik

Spectroscopy Institute, USSR Academy of Sciences
(Submitted 8 July 1980)
Zh. Eksp. Teor. Fiz. **80**, 1488–1503 (April 1981)

A procedure is developed to eliminate from the temperature diagram technique the divergences that occur in systems with degenerate ground states. The procedure is used to calculate rigorously the excitation spectrum and the correlation energy of a two-dimensional electron-hole system in a strong transverse magnetic field. If transitions to higher Landau levels are neglected, the system turns out to be an ideal exciton gas whose long-wave properties coincide with the properties of a two-dimensional Bose gas. Inclusion of the transitions leads to a weak (relative to a parameter) deviation from the ideal. The spectrum of the low-frequency excitations then becomes acoustic and the low-temperature behavior changes qualitatively. When the deviation from the ideal is taken into account, the topological phase transition with change of the asymptotic forms of the correlation functions, which is usual for two-dimensional degenerate systems, becomes possible in the system.

PACS numbers: 71.35. + z

1. INTRODUCTION

The main difficulties in the treatment, from first principles, of two-dimensional electron systems in transverse quantizing magnetic fields are due to the infinite degeneracy of the ground state. The usual diagram methods are not applicable at a temperature $T=0$, owing to the degeneracy. Diagram or operator methods especially developed for degenerate systems[1] are not always suitable: they yield secular equations which, without guessing the ground state, are not any easier to solve than the Schrödinger equation. On the other hand, degeneracy of any state imposes no limitation on the use of the temperature diagram technique, since the averaging is carried out over a grand canonical ensemble and the equality of the energies of certain states plays formally no role, even if the number of such states is infinite. In this case, however, almost all the diagrams turn out to be proportional to E_0/T (E_0 is the characteristic interaction energy), and at $T \ll E_0$ it is impossible to separate from the increasing diagrams the principal secondary sequence. This is precisely why the microscopic theory of two-dimensional electron or electron-hole ($e-h$) systems in strong magnetic fields was reduced up to now[2-5] to one variant of the Hartree-Fock approximation or another. The purpose of the present paper is to devise a temperature diagram technique free of the described difficulties and capable of rigorous account of the correlation effects in such systems.

Divergences (as $T \to 0$) can be avoided in the temperature diagram technique by partially including in the zeroth-approximation Hamiltonian $\mathscr{H}_0$ an interaction such that the degeneracy is lifted. The corresponding choice of the zeroth approximation in the case of a two-dimensional $e-h$ system in a strong magnetic field H is suggested by clear physical considerations. Since the spectrum of a two-dimensional exciton in a magnetic field is not degenerate,[6] the interaction that leads to exciton formation would have to be taken into account in the zeroth approximation. The simplest method would be to subdivide the electrons and holes into pairs, include the interaction in each pair in $\mathscr{H}_0$, and regard the interaction between particles from different pairs as a perturbation. In such an approach, however, the identity of the particles is not automatically preserved, and the ensuing difficulties are not offset by the lifting of the degeneracy. A method was therefore chosen different from the one described, but equivalent to it physically.

The zeroth approximation should be taken to be that of Hartree-Fock with $e-h$ pairing (its characteristics were calculated by us earlier). This approximation describes a coherent gas of excitons. The diagram technique is constructed in this case using matrix Green's functions whose off-diagonal components describe the $e-h$ pairing. All the diagrams converge as $T \to 0$, with any non-ladder diagram small relative to the parameter $(E_0/T) \cdot \exp(-E_0/2T)$. Neglecting transitions to higher Landau levels (whose contributions tends to zero as $H \to \infty$) the Hartree-Fock approximation turns out to be exact at $T=0$. At $T \neq 0$ the system is an ideal exciton gas with Bose long-wave characteristics. The correlation energy, described by vacuum ladder diagrams, is the free energy of the long-wave excitons, and the contribution made to the energy by the short-wave excitations is exponentially small. The properties of the system are therefore similar in this approximation to those of a two-dimensional ideal Bose gas.

Allowance for the higher Landau levels makes the exciton gas weakly ideal, thereby changing qualitatively its low-temperature properties. Thus, the heat capacity at the lowest temperatures is proportional to T^2, and at higher temperatures it becomes linear. (We note that in the absence of $e-h$ pairing the specific heat of the considered system is exponentially small as a function of temperature.[2]) Just as in other degenerate two-dimensional systems, the long-range order is destroyed by fluctuations. When account is taken of the weakly nonideality, however, a topological phase transition, accompanied by a change of the asymptotic behavior of the correlation and similar to the transition in two-dimensional Bose systems,[7,8] is possible in the system.

 0038-5646/81/040763-08$02.40

2. SELECTION OF DIAGRAMS AT HIGH TEMPERATURES

We consider a two-dimensional electron-hole plasma in a transverse magnetic field, with a Hamiltonian

$$\mathcal{H}=\sum_{\sigma=1,2}\int d^2\mathbf{r}\psi_\sigma^+(\mathbf{r})\hat{\xi}_\sigma\left(-i\frac{\partial}{\partial\mathbf{r}}+\frac{e}{c}\mathbf{A}\right)\psi_\sigma(\mathbf{r})$$
$$+\frac{1}{2}\sum_{\sigma,\sigma'=1,2}\int d^2\mathbf{r}d^2\mathbf{r}'\psi_\sigma^+(\mathbf{r})\psi_{\sigma'}^+(\mathbf{r}')\frac{\tilde{e}^2}{|\mathbf{r}-\mathbf{r}'|}\psi_{\sigma'}(\mathbf{r}')\psi_\sigma(\mathbf{r}), \quad (1)$$

where ψ_σ are the electron-annihilation operators in the band σ ($\sigma=1$ corresponds to the conduction band and $\sigma=2$ to the valence band; the electron representation of the operators is chosen in both bands), A is the vector potential of the uniform field H in the Landau gauge, $\tilde{e}^2\equiv e^2/\varepsilon$, ε is the effective permittivity, the electron dispersion laws are $\hat{\xi}_\sigma(p)=\pm(p^2/2m_\sigma-\mu)$, with the equal chemical potentials μ of the electrons and holes reckoned from the bottoms of the corresponding bands.

The fixed number N of electrons in the conduction band is equal to the number of holes in the valence band. We assume satisfaction of the condition

$$\rho\equiv N/N_0\leqslant 1, \quad (2)$$

wherein all particles are on the lower Landau level at the temperature $T=0$ [here $N_0=S/2\pi r_H^2$ is the Landau-level degeneracy multiplicity, S is the area of the system, $r_H=(c/eH)^{1/2}$ is the magnetic length, and $\hbar=1$]. The magnetic field is assumed strong,

$$r_H/a_0\ll 1, \quad (3)$$

so that we can neglect[2] the virtual transitions to higher Landau levels. Here $a_0=a_1+a_2$, $a_\sigma=1/m_0\tilde{e}^2$ is the effective Bohr radius in the band σ). For typical semiconductors, the condition (3) is satisfied in fields $H>10^5$ Oe.

The single-particle Green's function of a non-interacting $e-h$ gas is given in the Landau representations under conditions (2) and (3) by

$$G_\sigma(\omega, p_x; y, y')=g_\sigma(\omega)\chi_0(p_x, y)\chi_0(p_x, y'),$$
$$g_1(\omega)=-g_2(-\omega)=(i\omega+\mu_0)^{-1}, \quad (4)$$

where $\omega=\pi T(2k+1)$; $\chi_0(p_x, y)\equiv\chi_0(p_x r_H-y/r_H)$ are the oscillator wave functions of the electrons on the lower Landau level. It is convenient hereafter to refer the functions χ_0 to the bare vertex, which takes after integration over the y coordinates the form

$$\gamma(q_x, k_x)=\tilde{e}^2\int d\varkappa\frac{\exp[-(\varkappa^2+q_x^2)/2+ik_x\varkappa]}{(\varkappa^2+q_x^2)^{1/2}}. \quad (5)$$

Here q_x is the transferred (one-dimensional) momentum, k_x is the sum (or difference) momentum; all momenta are measured in units of $1/r_H$.

We consider second-order vertex diagrams (Fig. 1), where the solid lines denote the Green's functions g_1 and g_2 (and not $G_{1,2}$), and the dashed ones the interaction (5). The frequency parts of diagrams a-c (which, as in diagrams of any order, are calculated independently of the momentum parts) are

$$T^{-1}\delta_{\varepsilon 0}\rho(1-\rho), \quad (6)$$

where $\delta_{\varepsilon 0}$ is the Kronecker symbol. We have used here

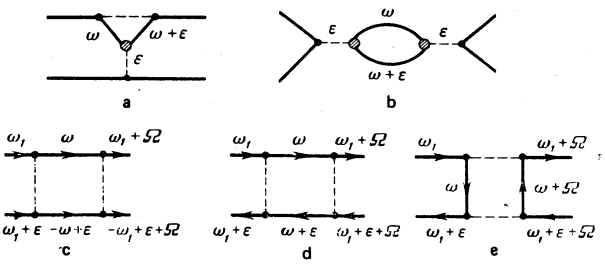

FIG. 1. Vertex diagrams of second order: at $T\geqslant T_0$, the solid lines are Green's functions of either the first or the second band; at $T<T_0$ each node corresponds to a band index σ; the solid line joining the nodes σ and σ' is the Green's function $g_{\sigma\sigma'}(\omega)$. The points denote fixed band indices (1 or 2), the shaded circle corresponds to summation over $\sigma=1$ and 2.

the condition that the number of particles is fixed[1)]:

$$N_0[\exp(-\mu_0/T)+1]^{-1}=N. \quad (7)$$

The momentum parts (i.e., the bare vertices) yield, after integration,[2)] factors $\sim E_0$, where

$$E_0=(\pi/2)^{1/2}\tilde{e}^2/r_H \quad (8)$$

is the binding energy of a two-dimensional exciton in a strong transverse magnetic field.[6] At

$$\alpha\equiv E_0T^{-1}\rho(1-\rho)\ll 1 \quad (9)$$

diagrams a-c give small corrections to the bare vertex (5). At low temperatures, on the contrary, these diagrams turn out to be significant. In higher orders of perturbation theory, the number of diagrams $\sim(E_0/T)^n$ increases, so that it is impossible to select diagrams as $T\to 0$. The reason is that the zeroth approximation was chosen to be the Hamiltonian of a non-interacting $e-h$ plasma in a magnetic field with ground-state degeneracy of infinite multiplicity.

Low temperatures will be considered in the next section. For the time being we confine ourselves to temperatures satisfying the condition (9). Under this condition the principal diagrams in all orders are the ladder $e-h$ diagrams, Fig. 1d. The total vertex function, corresponding to the sum of the ladder diagrams of this type (which describe the scattering of an electron from the first band by a hole from the second) is obtained from an integral equation that takes, after summation over the internal frequencies, the form

$$-\Gamma(\varepsilon; q_x, k_x)=\gamma(q_x, k_x)+\frac{1-2\rho}{i\varepsilon-2\mu_0}\int\frac{dq_x'}{2\pi}\gamma(q_x', k_x)\Gamma(\varepsilon; q_x-q_x', k_x).$$

This equation is easily solved in the transverse k-momentum representation introduced by Brazovskiĭ[9]:

$$\Gamma(\varepsilon, k)=\frac{1}{2\pi}\int\Gamma(\varepsilon; q_x, k_x)\exp(iq_xk_y)dq_x$$
$$=-E_0\gamma(k)\left\{1+\frac{E_0\gamma(k)(1-2\rho)}{i\varepsilon-2\mu_0+E_0\gamma(k)\,\mathrm{th}(\mu_0/2T)}\right\}, \quad (10)$$

$$E_0\gamma(k)=\frac{1}{2\pi}\int\gamma(q_x, k_x)\exp(iq_xk_y)dq_x=E_0\exp\left(-\frac{k^2}{4}\right)I_0\left(\frac{k^2}{4}\right), \quad (11)$$

where I_0 is a modified Bessel function. The transverse momentum k has the meaning of the exciton momentum[6] (introduced by Gor'kov and Dzyaloshinskiĭ[10] in the three-dimensional case). We shall need also the transverse q-momentum representation which is har-

monically conjugate to the k-representation. The bare vertex in the q representation is

$$\gamma(q)=\int\gamma(q_x,k_x)\exp(-ik_xq_y)\,dk_x=\frac{2\pi\tilde{e}^2}{q}\exp\left(-\frac{q^2}{2}\right). \qquad (12)$$

For an exciton, the quantity q has the meaning of the coordinate. The choice of the representation for the vertex is not unique, just as in the three-dimensional case.[9] Thus, the second-order ladder diagram (Fig. 1e), which is equivalent to diagram 1d with the input and output momenta interchanged, has a simple form in q-space. The total vertex (i.e., the sum of all the ladder diagrams of this type) also takes the form (10), (11) if the momentum k is replaced by q, and the sum frequency ε is replaced by the transferred frequency Ω. For such a vertex, the momentum q has the meaning of the exciton momentum.

When the temperature T is lowered, the pole at the vertex (10) appears first (at $k=\varepsilon=0$) at the temperature[3)]

$$T_0(\rho)=\frac{E_0}{2}\frac{1-2\rho}{\ln(\rho^{-1}-1)}. \qquad (13)$$

Continuing analytically the vertex (10) with respect to frequency into the upper half-plane (this reduces to the substitution $i\varepsilon\to\varepsilon+i0$), we can easily see that at $T<T_0$ the vertex (10) has on the real ε axis a pole corresponding to pairing of e and h. The pole points to the presence of exciton states with negative energy. Since the energy decreases when the excitons appear, it is necessary to reconstruct the ground state by taking the e–h pairing into account. At $T<T_0$ the vertex functions must be made up of single-particle Green's functions of the reconstructed state, which were obtained by us earlier[3] from the Gor'kov equations (in which is included, besides the anomalous vertex, also the normal Hartree-Fock vertex that describes the exchange interaction). This corresponds to a choice of the Hartree-Fock Hamiltonian (with allowance for e–h pairing) as the zeroth approximation.

3. SELECTION OF DIAGRAMS IN THE HIGH-TEMPERATURE REGION

We shall show that the ladder diagrams (of the type shown in Fig. 1d or 1e) are special also at $T\leqslant T_0(\rho)$. At these temperatures the Green's functions are the matrix quantities $g_{\sigma\sigma'}(\omega)$, and the off-diagonal components $g_{12}(\omega)$ correspond to pairing of an electron and a hole from different bands. Each node on the diagram is ascribed a band index σ (equal to 1 or 2), the solid line joining the nodes σ and σ' is $g_{\sigma\sigma'}(\omega)$, and the dashed line is the interaction (5), which is independent of the induces. The external band indices are fixed, and summation is carried out over the internal ones. The functions $g_{\sigma\sigma'}$ are given under conditions (2) and (3) by[3]

$$g_{11}(\omega)=-g_{22}(-\omega)=(-i\omega+\xi)(\omega^2+\eta^2)^{-1},$$
$$g_{12}(\omega)=g_{21}(\omega)=\Delta(\omega^2+\eta^2)^{-1}. \qquad (14)$$

Here Δ is the order parameter and is equal to zero at $T\geqslant T_0$; $\xi\equiv E_0\rho-\mu$, with the chemical potential $\mu=-E_0/2$ at $T>T_0$. At $T>T_0$ the potential μ is determined by the condition (7), in which μ_0 must be replaced by ξ; the parameter $\eta\equiv(\xi^2+\Delta^2)^{1/2}$ satisfies the equation

$$(E_0/2\eta)\,\mathrm{th}\,(\eta/2T)=1. \qquad (15)$$

[Expression (13) for T_0 was obtained earlier[3] from Eq. (15) under the condition $\Delta=0$.)

The frequency part of the diagram 1a, which describes the simplest correction to a triple vertex, is

$$T\sum_{\omega}g_{\nu\sigma}(\omega)g_{\sigma\mu}(\omega+\varepsilon)=\begin{cases}0, & \nu\neq\mu\\ -\dfrac{\delta_{\varepsilon 0}}{4T}\left(1-\mathrm{th}^2\dfrac{\eta}{2T}\right), & \nu=\mu.\end{cases} \qquad (16)$$

Summation over repeated indices is implied here and hereafter. The corresponding contribution of diagram 1b is obtained from (16) by summing over $\nu=\mu$. The momentum parts of these diagrams give the factors $\sim E_0^2$ (naturally, the same as at $T\geqslant T_0$). The diagrams 1a and 1b yield thus a correction of order α to the bare vertex, where

$$\alpha=\frac{E_0}{4T}\left(1-\mathrm{th}^2\frac{\eta}{2T}\right)\leqslant 1. \qquad (17)$$

At $T\ll E_0$ we obtain from (15)

$$\alpha=\frac{E_0}{T}\exp\left(-\frac{E_0}{2T}\right)\ll 1, \qquad (18)$$

so that the corrections to Figs. 1a and 1b are small. At $T=T_0$, when $\Delta=0$, the parameter (17) goes over into the parameter (9). The parameter (17) is consequently a parameter of the theory both at high temperatures (9) and at low ones (18). (The region of small α is shown in Fig. 2.) The ladder diagrams 1c and 1d have at low temperature no small quantity $\sim\alpha$. The diagrams 1c correspond to repulsion electron-electron interactions (intra- and interband). The excitations corresponding to ladder diagrams of this type are pure electron (or pure hole), so that in the long-wave limit they are certainly separated from the ground state by a gap. It is therefore necessary to sum ladder diagrams of the type 1d (or the equivalent diagrams 1e), which describe electron scattering by holes.

Since $\alpha\leqslant 1$ at all ρ or T, the selection of diagrams on the basis of these parameters makes it possible to obtain converging expansions in the entire considered

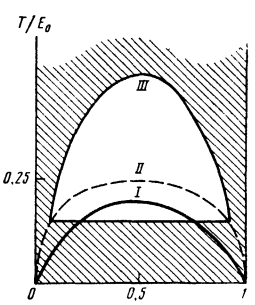

FIG. 2. Phase diagram of the system: line I marks the temperature of the Berezinskiĭ-Kosterlitz-Thouless transition (see Sec. 7). Its vertex corresponds to a temperature $T<E_0/4$, since ρ_s differs from ρ. Line II corresponds to the temperature $T_0(\rho)$. Line III is the arbitrary boundary on the phase plane between the regions of large and small α, with $\alpha<1/2$ on the shaded part. On the unshaded part, where $1/2\leqslant\alpha\leqslant 1$, the theory developed is only qualitatively applicable.

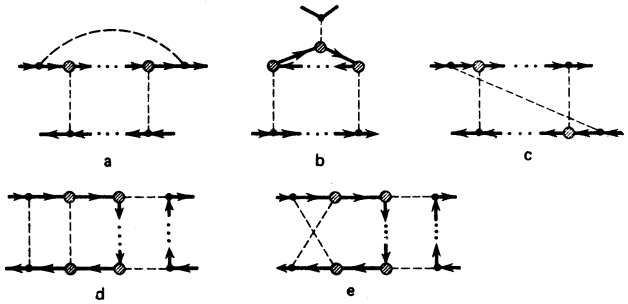

FIG. 3. Higher-order diagrams: the designations are the same as in Fig. 1.

region. Of course, the expansion will converge rapidly (and the selection will be well substantiated) in the region of small α (Fig. 2).

The parameter α is not bare (it is not proportional to the coupling constant). At $T < T_0$ a small factor appears in front of the diagram only after summation over the band indices. Each term (with definite band indices) is by far not small as $T \to 0$. For an arbitrary vertex diagram of order n, the number of such terms is 2^{2n-k} ($k=2,3,4$ is the number of fixed external indices of the diagram). Therefore before summing a ladder diagram we must verify that all the non-ladder diagrams of higher order are small. We divide the vertex non-ladder diagrams into reducible and irreducible. The reducible will include not only the vertices that are not cut by two fermion lines, but also those which break up after the cutting into two ladder blocks that do not contain a small quantity $\sim\alpha$. (In this sense the parquet diagram 3e is irreducible.) Obviously, it suffices to verify the smallness of the irreducible vertices.

We consider now irreducible diagrams containing a ladder block "spoiled" by only one non-ladder element (examples are Figs. 3a–c). The frequency parts of the diagrams 3a–b contain the sums

$$T\sum_{\bullet} g_{\sigma\sigma_1}(\omega+\varepsilon_1)g_{\sigma_1\sigma_2}(\omega+\varepsilon_2)\dots g_{\sigma_{n-1}\sigma'}(\omega+\varepsilon_n) \tag{19}$$

(with summation over repeated indices). It can be verified (e.g., by induction) that the following relation is valid:

$$g_{\sigma\sigma_1}(\omega+\varepsilon_1)g_{\sigma_1\sigma_2}(\omega+\varepsilon_2)\dots g_{\sigma_{n-1}\sigma'}(\omega+\varepsilon_n)$$
$$=\begin{cases}\dfrac{\eta+\xi}{2\eta}g^+(\omega+\varepsilon_1)\dots g^+(\omega+\varepsilon_n)+\dfrac{\eta-\xi}{2\eta}g^-(\omega+\varepsilon_1)\dots g^-(\omega+\varepsilon_n), & \sigma=\sigma'=1,\\ -\dfrac{\Delta}{2\eta}[g^+(\omega+\varepsilon_1)\dots g^+(\omega+\varepsilon_n)-g^-(\omega+\varepsilon_1)\dots g^-(\omega+\varepsilon_n)], & \sigma\neq\sigma',\end{cases} \tag{20}$$

where $g^{\pm}(\omega)=(i\omega\pm\eta)^{-1}$; at $\sigma=\sigma'=2$ it is necessary to reverse the sign of ξ in the upper line of the right-hand side of (20).

At $T=0$, the sums (19) reduce by virtue of formula (20) to integrals of the product of g^+ or g^- functions along the imaginary ω axis; these integrals vanish, since all the poles lie in the right (or left) complex half-plane. At $T\neq 0$ the sums (19) are represented by the integrals

$$\int_C \frac{d\omega}{2\pi}(\omega+i\varepsilon_1+\eta)^{-1}\dots(\omega+i\varepsilon_n+\eta)^{-1}\operatorname{th}\frac{\eta}{2T} \tag{21}$$

along the contour C that encloses the real axis. The sum of all the simple residues in (21) cancels out. This is easy to verify by noting that it is equal to zero at $T=0$, and the temperature dependence of an individual residue is given by $\tanh(\eta/2T)$. The sum of residues of order n is proportional to the derivative

$$\frac{d^{n-1}}{d\eta^{n-1}}\operatorname{th}\frac{\eta}{2T}\propto\frac{1}{T^{n-1}}\left(1-\operatorname{th}^2\frac{\eta}{2T}\right). \tag{22}$$

Since the n-th order residue appears when the arguments of n Green's functions coincide in (20), the resultant $n-1$ Kronecker symbols $\delta_{\varepsilon\varepsilon'}$ reduce the summation over the corresponding frequencies to multiplication by T, so that the factor $1/T^{n-1}$ in (22) cancels out as a result of this summation. A similar analysis shows that the diagrams 3c are likewise proportional to the parameter α, which appears, after two summations over the frequencies, in the form of the combination

$$\operatorname{cth}(\eta/T)-\operatorname{th}(\eta/2T). \tag{23}$$

The vertices containing more than one-ladder element (as the diagram 3e, made up of two ladders) can be treated similarly. It is sufficient to separate a chain of Green's functions of type (19), where the summation is over the frequency which does not enter in the arguments of the other Green's function (this is possible for the diagram 3e). An alternative is to separate two chains connected by a common frequency argument (as in diagram 3c), and then the small parameter appears in the form (23). This procedure can be used, at least in principle, to treat any diagram. Although it is impossible to prove in general form the smallness of any irreducible vertex, there are no grounds whatever to expect the appearance of some special vertex that does not have a small factor, since all the considered non-ladder diagrams (including those that are far from small in other $e-h$ systems[9,11]) are proportional to the parameter α. Since $\alpha=0$ in the limit of zero temperature and density, the amplitude for exciton-exciton scattering (described by non-ladder diagrams of the same structure as in the case of a three-dimensional exciton gas[11]) turns out to be zero. The considered exciton gas is consequently ideal (neglecting transitions to higher levels), as will be confirmed by an analysis that follows. This conclusion may seem unexpected, since the Pauli principle calls for the excitons to be repelled at distances $r \leqslant r_H$. In addition to repulsion, however, exchange attraction is also present. Both interactions are automatically taken into account in the formalism developed, and the deduction is that their contributions to the scattering amplitudes cancel out completely. This conclusion is confirmed by the equality of the exciton binding energy E_0 to the energy (per pair), calculated exactly in accord with the parameter r_H/a_0, of a closely packed $e-h$ system (when all the places on the lower Landau level are occupied: $N=N_0$, i.e., $\rho=1$).

4. CALCULATION OF THE VERTEX FUNCTION. EXCITATION SPECTRUM

To find the total vertex, neglecting the corrections in α, we must sum the ladder diagrams. In the transverse-momentum representation we obtain for the vertex Γ the linear system

$$\Gamma_{\alpha\beta,\mu\nu}(\mathbf{k},\varepsilon)=-E_0\gamma(\mathbf{k})\{\delta_{\alpha\beta}\delta_{\mu\nu}+\Xi_{\alpha\sigma,\tau\nu}(\varepsilon)\Gamma_{\sigma\beta,\mu\tau}(\mathbf{k},\varepsilon)\}, \tag{24}$$

where

$$\Xi_{\alpha\sigma,\tau\nu}(\varepsilon)=T\sum_{\omega} g_{\alpha\sigma}(\omega)g_{\tau\nu}(\omega+\varepsilon). \tag{25}$$

The system (24) breaks up into four systems of four equations each (one of them is shown in Fig. 4);

$$\begin{bmatrix} 1+\Xi_1\gamma & \Xi_2\gamma & \Xi_3\gamma & -\Xi_3\gamma \\ \Xi_2\gamma & 1+\Xi_1^*\gamma & \Xi_3^*\gamma & -\Xi_3^*\gamma \\ \Xi_3\gamma & \Xi_3^*\gamma & 1-\Xi_2\gamma & \Xi_2\gamma \\ -\Xi_3\gamma & -\Xi_3^*\gamma & \Xi_2\gamma & 1-\Xi_2\gamma \end{bmatrix} \begin{bmatrix} \Gamma_{1\beta,\mu 2} \\ \Gamma_{2\beta,\mu 1} \\ \Gamma_{1\beta,\mu 1} \\ \Gamma_{2\beta,\mu 2} \end{bmatrix} = -E_0\gamma(\mathbf{k}) \begin{bmatrix} \delta_{1\beta}\delta_{\mu 2} \\ \delta_{2\beta}\delta_{\mu 1} \\ \delta_{1\beta}\delta_{\mu 1} \\ \delta_{2\beta}\delta_{\mu 2} \end{bmatrix}. \tag{26}$$

The interaction (11) is designated here and elsewhere as $\gamma\equiv\gamma(\mathbf{k})$, $\Gamma\equiv\Gamma(\varepsilon,\mathbf{k})$. We used in (26) the identities

$$\begin{aligned} &\Xi_{11,22}(\varepsilon)=\Xi_1/E_0;\ \Xi_{12,12}(\varepsilon)=\Xi_2/E_0; \\ &\Xi_{11,11}(\varepsilon)=\Xi_{22,22}(\varepsilon)=-\Xi_2/E_0; \\ &\Xi_{12,22}(\varepsilon)=-\Xi_{11,12}(\varepsilon)=-\Xi_3/E_0; \\ &\Xi_{\alpha\beta,\mu\nu}(\varepsilon)=\Xi_{\beta\alpha,\mu\nu}(\varepsilon);\ \Xi_{\alpha\beta,\mu\nu}(\varepsilon)=\Xi_{\mu\nu,\alpha\beta}(-\varepsilon), \end{aligned} \tag{27}$$

where

$$\Xi_1=\frac{2(\xi^2+\eta^2+i\varepsilon\xi)}{\varepsilon^2+\eta^2};\quad \Xi_2=\frac{2\Delta^2}{\varepsilon^2+\eta^2};\quad \Xi_3=\frac{2\xi\Delta+i\varepsilon\Delta}{\varepsilon^2+\eta^2}.$$

In the calculation of the sums (25) we have discarded the corrections $\sim\alpha$. Solution of the system (26) yields the functions

$$\Gamma_{11,22}(\mathbf{k},\varepsilon)=-E_0\gamma\left\{1+2\gamma\frac{(\eta^2+\xi^2)(1-\gamma)+i\varepsilon\xi}{\varepsilon^2+4\eta^2(1-\gamma)^2}\right\} \tag{28}$$

$$\Gamma_{12,12}(\mathbf{k},\varepsilon)=-\gamma E_0-\Gamma_{11,11}(\mathbf{k},\varepsilon)=\frac{2E_0\Delta^2\gamma^2(1-\gamma)}{\varepsilon^2+4\eta^2(1-\gamma)^2}, \tag{29}$$

$$\Gamma_{11,12}(\mathbf{k},\varepsilon)=-E_0\gamma^2\frac{2\xi\Delta(1-\gamma)+i\varepsilon\Delta}{\varepsilon^2+4\eta^2(1-\gamma)^2}. \tag{30}$$

Vertex functions with other band indices are obtained from (28)–(30) with the aid of the symmetry relations (27). The analytic continuation of (28)–(30) into the upper ε half-plane is trivial. As a result we obtain the elementary excitation spectrum:

$$\mathscr{E}(\mathbf{k})=2\eta(1-\gamma)=E_0[1-\exp(-k^2/4)I_0(k^2/4)]. \tag{31}$$

We have used here the fact that, accurate to α, the parameter $\eta=E_0/2$. The dispersion law (31) coincides exactly with the dispersion law of an individual exciton[6] (reckoned from the binding energy $-E_0$), thus confirming again that the exciton gas is ideal. Asymptotic forms of $\mathscr{E}(\mathbf{k})$ are

$$\mathscr{E}(\mathbf{k})=\begin{cases} E_0k^2/4, & k\ll 1, \\ E_0-(2/\pi)^{1/2}E_0k^{-1}, & k\gg 1. \end{cases} \tag{32}$$

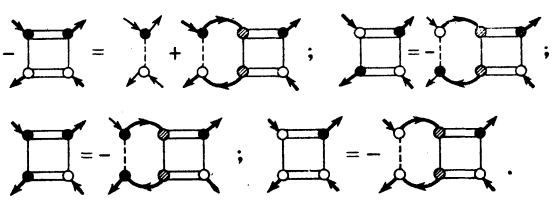

FIG. 4. Bethe-Salpeter equation for the vertex function: the black and white circles correspond to the band indices $\sigma=1$ and $\sigma=2$, respectively. Summation over $\sigma=1$ and 2 is carried out in the nodes with shaded circles. The equations given are for the functions $\Gamma_{\alpha 1,2\beta}$. The equation for the remaining Γ functions constitute similar systems.

($k\to kr_H$ in ordinary units.)

The vertices (28)–(30) have (after analytic continuation in ε) poles also at $\varepsilon=-\mathscr{E}(\mathbf{k})$. This is a consequence of the symmetry of the system with respect to the interchange $\rho\rightleftarrows 1-\rho$. At small ρ the excitations are ordinary excitons. At small $1-\rho$, when the lower Landau level is almost filled in the conduction band and almost empty (i.e., filled with holes) in the valence band, it is convenient to reckon the energy from that of the fully occupied Landau level. The excitations are then "anti-excitons" with negative dispersion law, made up of a hole in the conduction band and an electron in the valence band.

5. CORRELATION ENERGY

We analyze now the diagrams for the polarization operator. The single-loop operator

$$P_0(\varepsilon,\mathbf{q})=\frac{\delta_{\varepsilon 0}\alpha}{\pi E_0}\exp\left(-\frac{q^2}{2}\right) \tag{33}$$

is small in the parameter α. (The wave functions χ_0 are referred here to the Green's functions, and hence to the operator P_0 rather than to the interaction lines.) Since the ring diagrams diverge as $q\to 0$, they must be summed regardless of the factor α. The sum of these diagrams yield the correlation free energy in the random-phase approximation (RPA):

$$F_{RPA}=\pi TN_0\int\frac{d^2q}{(2\pi)^2}\left\{\ln\left[1+\frac{2\pi\tilde{e}^2}{q}P_0(0,\mathbf{q})\right]-\frac{2\pi\tilde{e}^2}{q}P_0(0,\mathbf{q})\right\}. \tag{34}$$

Equation (34), unlike the standard expression, contains no summation over the frequencies, owing to the factor $\delta_{\varepsilon 0}$ in (33). Simple transformations yield

$$F_{RPA}=-\frac{N_0T\alpha^2\ln\alpha}{\pi}=\frac{N_0E_0^3}{2\pi T^2}\exp\left(-\frac{E_0}{T}\right)\left[1+\frac{2T}{E_0}\ln\frac{T}{E_0}\right]. \tag{35}$$

The energy (35) is exponentially small. It is clear beforehand, however, that the ladder corrections to the polarization operator (33) must be substantial. The first correction to P_0 (Fig. 5a) turns out to be $\sim\alpha^2/E_0$, and the contribution made to the energy by diagrams

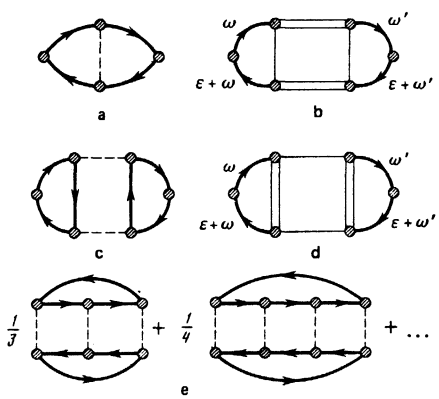

FIG. 5. Ladder corrections to the polarization operator (b, d) and the corresponding first approximations (a, c). The main contribution to the correlation free energy is given by the first-approximation diagrams in the operator of Fig. 5d, which is shown in the bare notation in Fig. 4. The contribution made to the energy by the diagrams with the operator of Fig. 5b is neglected.

with this polarization operator is negligible even compared with (35). Diagram 5a is the first approximation to diagram 5b. In the latter the vertex inset depends only on the frequency ε, and a summation, independent of ε, of the external Green's functions over the frequencies ω and ω' yields, just as in the first-order approximation, a factor α^2/E_0. The ladder inset 5d, in contast to that considered above, is quite significant. The polarization operator of Fig. 5d is given in the k-representation by

$$\Pi(\varepsilon,\mathbf{k})=T^2\sum_{\omega,\omega'} g_{\sigma\nu}(\omega)g_{\mu\sigma}(\omega+\varepsilon)\Gamma_{\nu\mu,\rho\tau}(\omega-\omega',\mathbf{k})g_{\tau\beta}(\omega')g_{\beta\rho}(\omega'+\varepsilon), \quad (36)$$

where, as in the preceding sections, the wave functions are referred to the bare vertices. After rather unwieldy summations we obtain from (36), using (27)–(30), the expression

$$\Pi(\varepsilon,k)=-\frac{2\alpha T\gamma}{\varepsilon^2+4\eta^2\gamma^2}\frac{\mathrm{sh}(\eta\gamma/T)}{\mathrm{sh}[\eta(1-\gamma)/T]} +\frac{\delta_{\sigma\sigma}\alpha}{4}\left[\frac{2}{\eta}\mathrm{cth}\left(\frac{\eta(1-\gamma)}{T}\right)-\frac{2-\alpha\gamma}{E_0}\right]. \quad (37)$$

Just as when the *RPA* diagrams are considered, it is convenient to refer the wave functions to the polarization operator rather than to the bare vertices. Then the correlation free energy is expressed in terms of the operator 5d by the following formula:

$$F_{corr}=T\sum_{\omega}\int\frac{d^2q}{(2\pi)^2}\int_0^1\frac{d\lambda}{\lambda}\frac{P(\varepsilon,\mathbf{q},\lambda)2\pi\tilde{e}^2\lambda/q}{1+P(\varepsilon,\mathbf{q},\lambda)2\pi\tilde{e}^2\lambda/q}, \quad (38)$$

where the polarization operator is

$$P(\varepsilon,\mathbf{q},\lambda)=\exp\left(-\frac{q^2}{2}\right)\int_0^\infty J_0(kq)\Pi(\varepsilon,k,\lambda)k\frac{dk}{2\pi}. \quad (39)$$

Here $\Pi(\varepsilon,k,\lambda)$ is given by (37), where each interaction function γ is multiplied by the coupling constant λ (J_0 is a Bessel function).

The main contribution to the energy (38) is made by the first approximation in $P(\mathbf{q})$ (i.e., by the sum of diagrams 5e). The formula for the free energy can be written in this approximation directly in the k-representation,[4)] without calculating the operator $P(\mathbf{q})$ (39):

$$F_{corr}=\frac{1}{2}N_0E_0T\sum_{\omega}\int_0^1 d\lambda\int_0^\infty\Pi(\varepsilon,k,\lambda)\gamma(k)k\,dk. \quad (40)$$

After summing over the frequencies and integrating with respect to the coupling constants we obtain from (40)

$$F_{corr}=N_0T\int_0^\infty\left\{\ln\left[\frac{\mathrm{sh}(\eta(1-\gamma)/T)}{\mathrm{sh}(\eta/T)}\right]+\frac{E_0}{T}\left(1+\frac{4\eta^2}{E_0^2}\right)\gamma+\frac{\alpha^2\gamma^2}{8}\right\}k\,dk. \quad (41)$$

At $k\gg 1$ (when $\gamma\ll 1$) the integrand is $\sim E_0\alpha^2\gamma^2/96T \sim 0.01E_0\alpha^2/k^3T$, so that a contribution proportional to $E_0\alpha^2$ is accumulated at large momenta k.

The main contribution to the energy (41) is made by integration over the small momenta $k\lesssim T/E_0\ll 1$. Neglecting the corrections $\sim\alpha^2$ in the integral over the small momenta, we obtain

$$F_{corr}=2N_0T\int_0^1\ln[1-e^{-2\eta u/T}]du=-N_0\frac{\pi^2T^2}{3E_0}, \quad (42)$$

and the result does not depend (accurate to α^2) on the upper limit that separates the small (compared with unity) momenta from the large ones.[5)]

It is important that the free energy (42) is independent of density, as are also any other correlation corrections to the free energy [including the *RPA* energy (35)]. Consequently, all corrections to the chemical potential $2\mu=-E_0$ are equal to zero. This is precisely why it was convenient to employ in the technique the variables N and T (rather than μ and T), for then the sum of the vacuum diagrams yields the free energy (and not the Ω-potential).

The free energy (42) can be obtained as the energy of the long-wave (with momenta $k\ll 1$) excitations (32) if it is assumed that they are described by Bose statistics. (Of course, short-wave excitons do not obey Bose statistics: if this statistics is applied to the entire spectrum (31) we obtain not the correct (converging) formula (41), but an expression that diverges as $k\to\infty$.)[6)] Consequently, neglecting transitions to higher Landau levels, the system behaves indeed as an ideal Landau gas of quasi-zero-dimensional excitons, and the long-wave properties of this gas coincide with those of an ideal two-dimensional Bose gas. The free energy (42) is the energy of the above-condensate excitations, which vanishes at $T=0$. This energy is small (in the parameter $T/E_0 \leqslant \frac{1}{4}$) compared with the Hartree-Fock free energy[3]:

$$F_{HF}(\rho,T)=\frac{\rho_0(T)}{\rho}F_{eh}[\rho_0(T),T]-\left[1-\frac{\rho_0(T)}{\rho}\right]E_0, \quad (43)$$

where $F_{eh}(\rho)$ is the free energy per e–h pair at $T\geqslant T_0$:

$$F_{eh}(\rho,T)=-E_0\rho+2T[\ln\rho+(\rho^{-1}-1)\ln(1-\rho)], \quad (44)$$

and $\rho_0(T)$ is either solution (of the two) of Eq. (13) for ρ at fixed $T\leqslant E_0/4$.

At $T=0$, when all the correlation corrections are equal to zero, Eqs. (43) and (44) are exact. Despite the smallness of the free excitation energy (42) compared with the energy (43), a number of thermodynamic properties are determined precisely by expression (42). Thus, the specific heat at constant volume, determined by the energy (43), is exponentially small if the theory (18) is valid, whereas the specific heat of the above-condensate excitations, determined from (42), is proportional to T: under condition (9) the correlation pressure turns out to be larger than the Hartree-Fock pressure.

6. TWO-DIMENSIONAL DIVERGENCES

We have ignored so far the divergences in the considered two-dimensional system. It is clear from the calculation of the correlation energy that as $k\to 0$ the momentum tends to have a Bose distribution function

$$N_k=\left[\exp\left(\frac{E_0k^2-\zeta}{T}\right)+1\right]^{-1} \quad (45)$$

with a zero chemical potential ζ. (This result can be easily obtained directly.) Since the function (45) is not integrable at the lower limit at $T=0$ (in two-dimensional space), no excitation condensate can exist at nonzero temperatures. Just as in an ideal two-dimensional Bose gas, the condensate is destroyed by the fluctuations of the density rather than those of the phase of the order parameter. (In the system considered here this is true only if the corrections in r_H/a_0 are neglected.)

No phase transition whatever is therefore possible in the system in this approximation.

Expression (42) for the correlation free energy, obtained in the preceding section (under the assumption that the condensate exists) is valid despite the absence of a condensate. The point is that the chemical potential ζ of the elementary-excitation gas, while not zero (as would be in the case of condensation), is small as $T \to 0$, so that the energy (42) remains constant accurate to $\exp(-E_0/T)$. Since the condensate is destroyed by long-wave fluctuations and the free energy is determined only by long-wave excitations, it suffices to demonstrate the validity of (42) for an ideal Bose gas with the same long-wave properties as the considered exciton gas. The chemical potential ζ and the free energy F of an ideal gas with a spectrum $E_0k^2/4$ and a distribution (45) are given by

$$\rho = (2T/E_0) g_1(-\zeta/T), \tag{46}$$

$$F = -2N_0T^2E_0^{-1}g_2(-\zeta/T) + \zeta N_0\rho, \tag{47}$$

where

$$g_n(x) = \sum_{m=1}^{\infty} e^{-mx} m^{-n}$$

is an integral Bose function. At $\rho > \frac{1}{2}$ we must replace ρ in (46) and (47) by $1-\rho$. At $T \ll E_0\rho$ [or respectively $T \ll E_0(1-\rho)$], using the asymptotic formulas[12] for $g_n(x)$, we obtain ζ from (46) in the form

$$\zeta = -T \exp(-\rho E_0/2T),$$

after which expression (47), accurate to exponentially small terms, goes over into (42).

In a number of thermodynamic quantities, the singularities (that would exist in the case of condensation) are preserved in a "smoothed" form. Thus, the isothermal compressibility and the specific heat c_P are finite also at $T < T_0$, but increase exponentially under the condition (18) (and become infinite at $T = 0$). The specific heat c_v has at $T \sim T_0$ a maximum (rather than the kink at $T = T_0$ in the case of condensation).

7. CHANGE OF LONG-WAVE CHARACTERISTICS WHEN HIGHER LANDAU LEVELS ARE TAKEN INTO ACCOUNT

Inclusion of the higher Landau level leads to weak nonideality of the exciton gas and this changes qualitatively its long-wave (and hence low-temperature) behavior. Since the corrections in the small parameters r_H/a_0 and α are additive, we consider at present only the corrections connected with transitions to higher Landau levels, and assume that $\alpha = 0$.

It is easily seen that at $T = 0$ each order in the interaction yields a factor r_H/a_0 in the diagrams for the correlation energy so that it suffices to retain diagrams of the lowest second order. The contribution of these diagrams to the energy (per $e-h$ pair) is

$$\Delta E = -\alpha_1 E_0 \rho, \tag{48}$$

and this energy does not depend on the $e-h$ pairing.[3] (Here $\alpha_1 = 0.13 r_H/a_0$.) It must be recognized that the Hartree-Fock energy (43) also changes when account is taken of transitions to higher levels. The left-hand side of the compatibility Eq. (15) must be multiplied by $(1+\alpha_2)$, where $\alpha_2 = 0.29 r_H/a_0$, and the chemical potential of the exciton phase changes as a result. The total energy change at $T = 0$ is

$$F_0/N = -\alpha_2 E_0(1-\rho) - \alpha_1 E_0 \rho. \tag{49}$$

The compressibility at $T = 0$ is therefore

$$\varkappa = V^{-1}\frac{\partial^2 V}{\partial F_0^2} = \frac{\pi r_H^2}{E_0\rho^2(\alpha_2 - \alpha_1)}.$$

The compressibility thus turns out to be finite also at $T = 0$, but still quite large—inversely proportional to the small parameter r_H/a_0. One can therefore expect to observe in experiment a practically critical opalescence that increases with increasing H and with decreasing T. The sound velocity c is obtained from (49) in the form

$$c = E_0 r_H [\rho(\alpha_2 - \alpha_1)]^{1/2}. \tag{50}$$

At $T = 0$ the spectrum and the correlation energy can be calculated from the same diagrams that were used to calculate them above without allowance for the corrections in r_H/a_0. It is clear beforehand, however, that the spectrum is acoustic at momenta $kr_H \lesssim k_0 \ll 1$ and quadratic in the interval $k_0 \lesssim kr_H \lesssim 1$. The order of magnitude of the momentum k_0 is determined by the energy-matching condition $ck_0 \sim E_0 k_0^2 r_H^2$, whence $k_0 r_H \sim (\rho r_H/a_0)^{1/2}$. At temperatures $T \gtrsim ck_0$ the free energy is determined by the quadratic part of the excitation spectrum, but formula (42) remains valid for it. At

$$T \lesssim ck_0 \sim \rho E_0 r_H/a_0 \tag{51}$$

the free energy is the energy of the acoustic excitations, for which we obtain in the usual manner

$$F = -N_0 T^3 r_H^2 c^{-2} \zeta(3) \tag{52}$$

[$\zeta(3) = 1.20$ is a Riemann zeta function].

In the region (51) the specific heat determined from (52) is quadratic in the temperature, and at $ck_0 \lesssim T \lesssim E_0/4$ the growth of the specific heat becomes linear in accord with (42). The temperature (51) that separates the quadratic growth from the linear decreases with increasing H.

At $kr_H \lesssim 1$ the momentum distribution function remains, naturally, of the Bose type, but at $k \lesssim k_0 \ll r_H^{-1}$ it has an acoustic spectrum. Long-range order in the system is impossible, but, just as in a weakly ideal gas, it is destroyed by fluctuations of the phase of the order parameter. A topological phase transition therefore becomes possible, with a change of the asymptotic behavior of the correlation functions from exponential to power-law, in analogy with the transitions in other degenerate two-dimensional systems.[7,8]

The low-temperature characteristics of the transitions are determined entirely by the low-lying excitations, which in the considered system are of the Bose type (accurate to exponentially small quantities). Therefore the formulas that describe the transition coincide with those for two-dimensional Bose systems.[7,8] There is only one substantial difference, due to the already mentioned symmetry of the considered system

relative to replacement of ρ by $1-\rho$. [At first glance this symmetry is violated in Eq. (49), which describes the corrections in r_H/a_0, since $\alpha_1 \neq \alpha_2$. This inequality, however, ensures a correct (positive) sign of the compressibility of the exciton gas and a negative sign of the equal (in absolute value) compressibility of the gas of antiexcitons, with negative dispersion law.] The collective acoustic excitations can be regarded as excitations in an exciton gas at small ρ or in an antiexciton gas at small $1-\rho$. The formula for the transition temperature can therefore be written in the form

$$T_c = \frac{\pi\rho_s(1-\rho_s)}{2\pi r_H^2 M_0} = E_0\rho_s(1-\rho_s). \qquad (53)$$

Here $\rho_s = N_s/N_0$ is the superfluid density.

At low T, the only ones for which (53) is valid, we have $\rho_s \approx \rho$. A plot of T_c is shown in Fig. 2, from which it is seen once more that (53) is valid only at $\rho(1-\rho) \ll 1$. Since the speed of sound does not enter in (53), this expression describes formally also the case of an ideal gas ($c=0$). In reality the transition vanishes as $c \to 0$. This follows formally from the vanishing, at $c=0$, of the cutoff parameter $r_0 = c/T$ in the asymptotic form of the correlation function.[7] Physically, owing to the infinite growth of the size and of the decrease of the energy of the vortices in the Bose gas as $c \to 0$,[13] it is clear that a topological phase transition is impossible at $c=0$.

[1)] In Fig. 1 there are no diagrams describing the Hartree-Fock (exchange) corrections to the Green's functions. The summation of all such diagrams[2] leads to replacement of μ^0 in the Green's functions (4) 0, where $\varepsilon 0 = -\varepsilon 0\rho$ is the renormalization of the energy of the lower Landau level. However, ξ will replace $-\mu_0$ also in the condition (7), so that expression (6) (and the other estimates of that section) will not change if the Hartree-Fock approximation (without e-h pairing) is taken to be the zeroth approximation and the bare Green's functions are replaced by Hartree-Fock functions.

[2)] Divergences at small momenta in ring diagrams (of the type shown in Fig. 1b) are eliminated by summing these diagrams in all orders, as will be shown in Sec. 5.

[3)] We emphasize that the selection of diagrams in accord with the parameter (9) at $T \geqslant T_0$ is valid up to $T = T_0$. At $T = T_0(\rho)$ the parameter α is equal to 1 only at $\rho = 1/2$ (when $T_0 = E_0/4$), and at all other $\rho < 1$ we have $\alpha < 1$, with $\alpha \to 0$ as $\rho \to 0$ or $1-\rho \to 0$.

[4)] We note once more the full equivalence of the **k** and **q** spaces. The operator P could be obtained in the **q** representation by taking the upper insets in the form shown in Fig. 1e. The energy F would then be given by Eq. (38) in terms of the operator P in the **k** representation. The interchange of the representations reduces here to the transformation $\mathbf{q} \rightleftarrows \mathbf{k}$.

[5)] The contribution of any finite number of vacuum ladder diagrams (Fig. 5e) is $\sim E_0\alpha^2$. The exponentially small factor is offest by summing the entire series of such diagrams. But even the first diagram of the series makes a contribution of the same order as F_{KPA} to the free energy.

[6)] That Bose statistics does not hold for excitations with $k \gtrsim 1$ is clear from the following considerations: just as in the three-dimensional case,[10] the distance between the electron and hole constituting the exciton is equal to k (kr_H^2 in the usual units),[6] so that at $k \gtrsim 1$ the Fermi character of the electron and of the hole that make up the exciton manifests itself.

[1]T. Morita, Progr. Theor. Phys. **29**, 351 (1963). D. A. Kirzhnits, Polevye metody teorii mnogikh tel (Field Methods of Many-Body Theory), Gosatomizdat, 1963. L. N. Bulaevskiĭ, Zh. Eksp. Teor. Fiz. **51**, 230 (1966) [Sov. Phys. JETP **24**, 154 (1967)]. G. M. Vagradov, FIAN Preprint, 1965.

[2]I. V. Lerner and Yu. E. Lozovik, Sol. St. Comm. **23**, 453 (1977); Zh. Eksp. Teor. Fiz. **74**, 274 (1978) [Sov. Phys. JETP **47**, 140 (1978)].

[3]I. V. Lerner and Yu. E. Lozovik, Pis'ma Zh. Eksp. Teor. Fiz. **27**, 497 (1978) [JETP Lett. **27**, 467 (1978)]; Low Temp. Phys. **38**, 333 (1980).

[4]Y. Kuramoto and C. Horie, Sol. St. Comm. **25**, 713 (1978).

[5]H. Fukuyama, P. M. Platzman, and P. W. Anderson, Phys. Rev. **19B**, 5211 (1979). D. Yoshioka and H. Fukuyama, J. Phys. Soc. Japan **47**, 394 (1979).

[6]I. V. Lerner and Yu. E. Lozovik, Zh. Eksp. Teor. Fiz. **78**, 1167 (1980) [Sov. Phys. JETP **51**, 588 (1980)].

[7]V. L. Berezinskiĭ, *ibid.* **59**, 907 (1970); **61**, 1144 (1971) [32, 493 (1971); **34**, 610 (1972)].

[8]J. M. Kosterlitz and D. I. Thouless, J. Phys. **C6**, 1181 (1973). J. M. Kosterlitz, *ibid.* **C7**, 1046 (1974).

[9]S. A. Brazovskiĭ, Zh. Eksp. Teor. Fiz. **61**, 2401 (1971); **62**, 820 (1972) [Sov. Phys. JETP **34**, 1286 (1972); **35**, 433 (1972)].

[10]L. P. Gor'kov and I. E. Dzyaloshinskiĭ, *ibid.* **53**, 717 (1967) [**26**, 449 (1968)].

[11]L. V. Keldysh and A. N. Kozlov, *ibid.* **54**, 978 (1968) [**27**, 521 (1968)].

[12]J. E. Robinson, Phys. Rev. **83**, 678 (1951).

[13]E. M. Lifshitz and L. P. Pitaevskiĭ, Statisticheskaya fizika (Statistical Physics), part II, Nauka, 1979.

Translated by J. G. Adashko